Geophysical Research Letters

RESEARCH LETTER
10.1029/2022GL102340

Key Points:

- Temporally stable climate response to increased sea salt aerosol in GFDL's AM4 and CM4 models following the G4sea-salt protocol
- Dominant role of direct aerosol effects in both models as the indirect aerosol–cloud effects are counterbalanced by cloud feedbacks in CM4
- Uncertain spatial radiative and cloud responses necessitating further constraining to yield detailed mechanistic understanding

Supporting Information:

Supporting Information may be found in the online version of this article.

Correspondence to:

N. G. A. Mahfouz,
nm2266@princeton.edu

Citation:

Mahfouz, N. G. A., Hill, S. A., Guo, H., & Ming, Y. (2023). The radiative and cloud responses to sea salt aerosol engineering in GFDL models. *Geophysical Research Letters*, *50*, e2022GL102340. https://doi.org/10.1029/2022GL102340

Received 29 NOV 2022
Accepted 9 JAN 2023

Author Contributions:

Conceptualization: Naser G. A. Mahfouz, Yi Ming
Data curation: Naser G. A. Mahfouz
Formal analysis: Naser G. A. Mahfouz, Spencer A. Hill
Funding acquisition: Yi Ming
Investigation: Naser G. A. Mahfouz
Methodology: Naser G. A. Mahfouz, Huan Guo
Project Administration: Yi Ming
Software: Naser G. A. Mahfouz, Huan Guo
Supervision: Spencer A. Hill, Yi Ming
Validation: Naser G. A. Mahfouz
Visualization: Naser G. A. Mahfouz

The Radiative and Cloud Responses to Sea Salt Aerosol Engineering in GFDL Models

Naser G. A. Mahfouz[1], Spencer A. Hill[1,2], Huan Guo[3], and Yi Ming[3,4]

[1]Atmospheric and Oceanic Sciences, Princeton University, Princeton, NJ, USA, [2]Lamont-Doherty Earth Observatory, Columbia University, Palisades, NY, USA, [3]NOAA Geophysical Fluid Dynamics Laboratory, Princeton, NJ, USA, [4]Schiller Institute for Integrated Science and Society, Department of Earth and Environmental Sciences, Boston College, Boston, MA, USA

Abstract Marine cloud brightening is a proposal to counteract global warming by increasing sea salt aerosol emissions. In theory, this increases the cloud droplet number concentration of subtropical marine stratocumulus decks, increasing cloud brightness and longevity. However, this theoretical progression remains uncertain in coupled climate models, especially the response of liquid water path and cloud fraction to aerosol seeding. We use the GFDL CM4 climate model to simulate marine cloud brightening following the published G4sea-salt protocol, in which sea salt aerosol emissions are uniformly increased over 30 S–30 N in addition to standard forcings from a SSP2-4.5 future warming scenario. The perturbed radiative and cloud responses are temporally stable though spatially heterogeneous, and direct scattering by the added sea salt predominates over changes to cloud reflectance. In fact, feedbacks in the coupled simulation lead to a net warming, rather than cooling, response by clouds.

Plain Language Summary With calls for climate action rising, some countries and groups may be looking at counteracting global warming. As reducing emissions of greenhouse gases remains elusive, and while the results of climate change manifest in extreme events and weather records, state or private actors may look for active engineering solutions which remain hypothetical and not fully scientifically understood. Using premier climate models at NOAA GFDL, we examine one form of climate engineering, marine cloud brightening, aimed at increasing radiation reflected back to space by increasing sea salt aerosol emissions in the marine tropics. We find the climate response to a protocol of this scheme temporally stable over the time period of the simulation, though spatially uncertain. Moreover, the response is largely dominated by effects resulting from the direct interactions between aerosol particles and solar radiation, and not via clouds. Our results paint a more nuanced picture than previous studies and as such raise more questions and uncertainties about proposals for marine cloud brightening, at least through the prism of state-of-the-art climate models.

1. Introduction

Solar climate engineering, or geoengineering, refers to slowing anthropogenic climate change by increasing planetary albedo (National Academies of Sciences, Engineering, and Medicine, 2021). Example proposals include increasing direct scattering of insolation through stratospheric aerosol injection and, our focus, marine cloud brightening (MCB). As MCB is envisioned, sea salt aerosol (SSA) emissions would be increased in order to increase cloud droplet number concentrations (CDNCs) within the subtropical marine stratocumulus decks, thereby increasing cloud albedo and longevity through the aerosol indirect effects (Latham & Smith, 1990; Latham et al., 2012).

Because it relies on uncertain aerosol–cloud interactions (Sherwood et al., 2020; Stocker, 2014), MCB has been challenging to comprehensively study in climate models. The added particles must be small enough to avoid increasing precipitation, but large enough to activate into cloud droplets. Many modeling studies, such as those following the G4cdnc protocol (Kravitz et al., 2013), sidestep these aerosol–cloud interaction uncertainties by simply prescribing increases in boundary-layer CDNC (e.g., Jones et al., 2009; Kim et al., 2020; Rasch et al., 2009; Stjern et al., 2018; Zhu et al., 2021). Others, by prescribing an increase in SSA number concentration rather than CDNC, include the aerosol–cloud interactions but not the processes involved in going from the SSA emissions to SSA burdens (S. Hill & Ming, 2012; Jones & Haywood, 2012; Partanen et al., 2012).

Writing – original draft: Naser G. A. Mahfouz
Writing – review & editing: Naser G. A. Mahfouz, Spencer A. Hill, Huan Guo, Yi Ming

The full chain of processes starting from the SSA emissions are included in the G4sea-salt (Kravitz et al., 2013) and another (Adeniyi & Bassey, 2021; Alterskjaer et al., 2013) protocol. In both, emission rates of SSA are increased in otherwise standard future warming scenario simulations by an amount that generates a specified negative global-mean effective radiative forcing (ERF). Yet, there has been considerably less study of these compared to the prescribed-aerosol or prescribed-CDNC simulations. Ahlm et al. (2017) compare the results of G4sea-salt in three Earth system models, finding—consistent with all the aforementioned perturbed-SSA-emission and perturbed-SSA-burden simulation studies—that the direct scattering effect of the SSA plays a significant role in the radiative offset (as deduced from the clear-sky radiative component), despite the intended cooling mechanism being through enhanced cloud albedo.

We investigate the aerosol and cloud microphysical uncertainties in MCB by simulating the G4sea-salt protocol in NOAA GFDL models. We find that not only do the direct effects play a dominant role in forcing the net cooling response, the cloud response in the coupled simulation counteracts this globally averaged cooling effect, acting to warm rather than cool the surface.

2. Methods

We implement G4sea-salt in GFDL models, namely the coupled model, CM4, and its atmosphere component, AM4. Four separate simulations are conducted, for each model with and without additional SSA emissions. We first describe the GFDL models in Section 2.1, outline the implementation of G4sea-salt in Section 2.2, and finally detail our analysis methods in Section 2.3.

2.1. Model Description

The GFDL AM4 atmospheric model (Zhao et al., 2018a, 2018b) employs a cubed-sphere topology with 96 × 96 grid boxes on each of its six faces, corresponding to ∼100 km horizontal resolution. It has 33 levels ending at 1 hPa, including an additional near-surface layer (Shin et al., 2019). The cloud macrophysics follows Rotstayn (1997) and Rotstayn et al. (2000) in treatment of source and sink cloud condensates with a prognostic scheme for CDNC by Ming et al. (2007).

Surface emission of SSA follows Mårtensson et al. (2003) for particles smaller than 1.4 μm and Monahan et al. (1986) for larger particles, the former depending on both sea surface temperature (SST) and wind speeds while the latter only on wind speeds (e.g., Spada et al., 2013). SSA particles are grouped into five size bins from 0.1 to 10 μm of dry radius (Paulot et al., 2020). Hygroscopic growth of SSA and their refractive indices follow Tang et al. (1997). Aerosol activation into cloud droplets follows Ming et al. (2006, 2007), and their efficiency as cloud condensation nuclei is assumed to be the same as that of pure sodium chloride particles.

The cloud activation scheme redistributes the submicron mass of SSA particles present onto a prescribed size distribution (Ming et al., 2006, 2007). The prescribed size distribution has three distinct modes with predefined total number concentration ratio in cm^{-3} (340:60:0.75), diameter geometric means (10, 150, and 620 nm), and geometric standard deviations (1.6, 2.0, and 2.7) held constant (respectively for all). Note this fixed modal representation using three modes for liquid cloud activation and thus indirect effects contrasts with the fixed sectional representation using five bins used for emissions and thus direct effects.

The CM4 coupled model (Held et al., 2019) consists of AM4 coupled to the LM4 land model (Zhao et al., 2018b) and the OM4 ocean model (Adcroft et al., 2019). OM4 uses a horizontal resolution of 0.25° with 75 layers.

2.2. Simulation Protocol

We first run the coupled model, CM4, following the standard Shared Socioeconomic Pathway 2-4.5 (SSP2-4.5) forcing scenario from 2020 to 2090. We then run two fixed-SST simulations in AM4, with annual-mean SSTs from year 2020 of the CM4 SSP2-4.5 simulation. All radiative forcing agents in the AM4 simulations are kept at their 2020 values, except in one where the SSA emissions are perturbed as follows. Under the G4sea-salt protocol, SSA emissions are increased by a uniform absolute rate over all lowermost ocean grid points 30°S–30°N to generate a global-mean shortwave radiative offset of -2 W m^{-2} (Kravitz et al., 2013), determined via the radiative flux perturbation method (Hansen, 2005; Rotstayn, 2005). The value needed for the desired radiative offset is

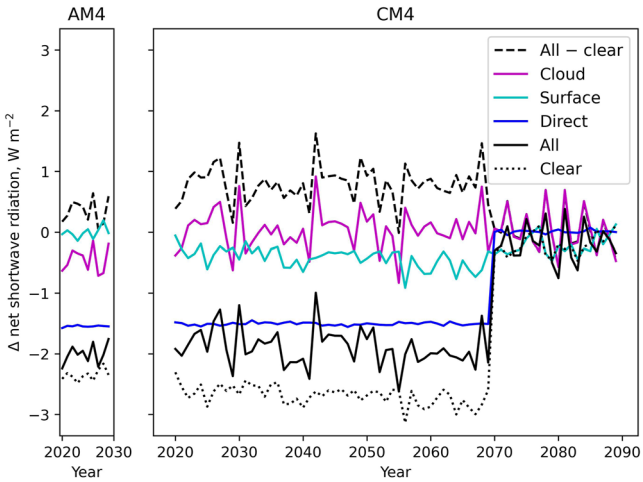

Figure 1. Annual global-means shortwave radiation imbalance atop the atmosphere (SWR TOA) from the fixed-sea surface temperature simulation (2020–2030) and the coupled simulation (2020–2090). The all-sky (All) radiation is decomposed into the conventional clear-sky (Clear) and the difference between all-sky and clear-sky (All − Clear) as well as into the Ghan (2013) components: the cloud radiative (Cloud), surface albedo (Surface), and direct radiative (Direct) effects.

7.66×10^{-11} kg m^{-2} s^{-1}, determined iteratively through several short fixed-SST runs. Finally, we run the coupled model CM4 again following SSP2-4.5 but with additional SSA emissions from 2020 to 2070. At 2070, the SSA emission modification is abruptly turned off and the integration continues to 2090 to study termination effects.

Kravitz et al. (2013) recommend injecting particles in a loosely defined "accumulation mode" citing Alterskjær and Kristjánsson (2013), who show the most effective modal size is 0.13 μm with the geometric standard deviation of 1.59. In AM4, this roughly corresponds to the first two bins, 0.1–0.5 μm and 0.5–1 μm in dry radius. As such, we increase the emission rate by a fixed absolute mass flux rate in these two bins only. The design choice to use the first two bins in GFDL models allows us to perturb all particles used in the cloud activation scheme, and thus offers the best available comparison vis-a-vis the direct effects and other previous studies. We note that much smaller sizes are likely needed for MCB to be effective (e.g., Ahlm et al., 2017; Hoffmann & Feingold, 2021; Wood, 2021), but this remains an active area of research.

2.3. Analysis Methods

We decompose the net shortwave radiation imbalance atop the atmosphere (SWR TOA) into the conventional components, all sky, clear sky, and the difference thereof, where the clear-sky part is calculated in the absence of clouds. To have a more accurate representation of the radiative components, we additionally follow Ghan (2013) to decompose the SWR TOA into direct radiative effects, cloud radiative effects, and the surface albedo effects. The latter approach by Ghan (2013) accounts for cloud masking and is obtained using additional calls to the radiative transfer code with and without aerosols, on top of the conventional calls with and without clouds. (See Text S2 in Supporting Information S1 for more information.)

We use three cloud properties in this study. We represent CDNC by its maximum value in the layers below 850 mb following Ahlm et al. (2017). Liquid water path (LWP) is calculated, as usual, by an integration of the liquid content in the atmospheric column. The low cloud fraction is the cloud fraction under atmospheric layers below 680 mb following Rossow and Schiffer (1999).

For long-term averages, in the AM4 simulations we use the full 10-year duration, and for the CM4 simulations we use years 2035–2065. In all cases, we show the difference between the perturbed simulations and the reference simulations, that is, $\Delta V = V_{\mathrm{G4S}} - V_{\mathrm{SSP}}$ for value V of interest. We apply Welch's adaptation (Welch, 1947) of Student's t test statistics with the null hypothesis of no difference in the mean of the two samples (one-tailed).

3. Results

3.1. Radiative Imbalance

The net global-mean SWR TOA flux anomaly timeseries in AM4 is shown in Figure 1, signed positive downward. Because the global-mean longwave response in AM4 is negligible (time-mean +0.025 W m^{-2}), the SWR TOA (−2.00 W m^{-2}) is approximately equal to the inferred global-mean ERF. Figure 1 also includes the global-mean decomposition of the SWR TOA into components following the conventional clear-sky breakdown (time-mean −2.35 for the clear sky and thus +0.35 W m^{-2} for the difference between all sky and clear sky) as well as into the Ghan (2013) terms (time-mean −0.45, −0.01, and −1.54 W m^{-2} for the cloud radiative, surface albedo, and direct radiative effects, respectively). For all terms, interannual variability is modest and there is no indication of a long-term trend, lending confidence to the accuracy of the time-mean values as approximations to the ERF and its components.

The spatial distributions of the time-mean SWR TOA forcing and its components are shown in the left column of Figure 2. Unsurprisingly given the imposed SSA emission perturbation only over the tropical oceans, the total signal (panel i) is strongest and predominantly negative over the tropical oceans, especially over the stratocumulus regions west of subtropical continents, with more spatial noise and overall less negative responses over tropical

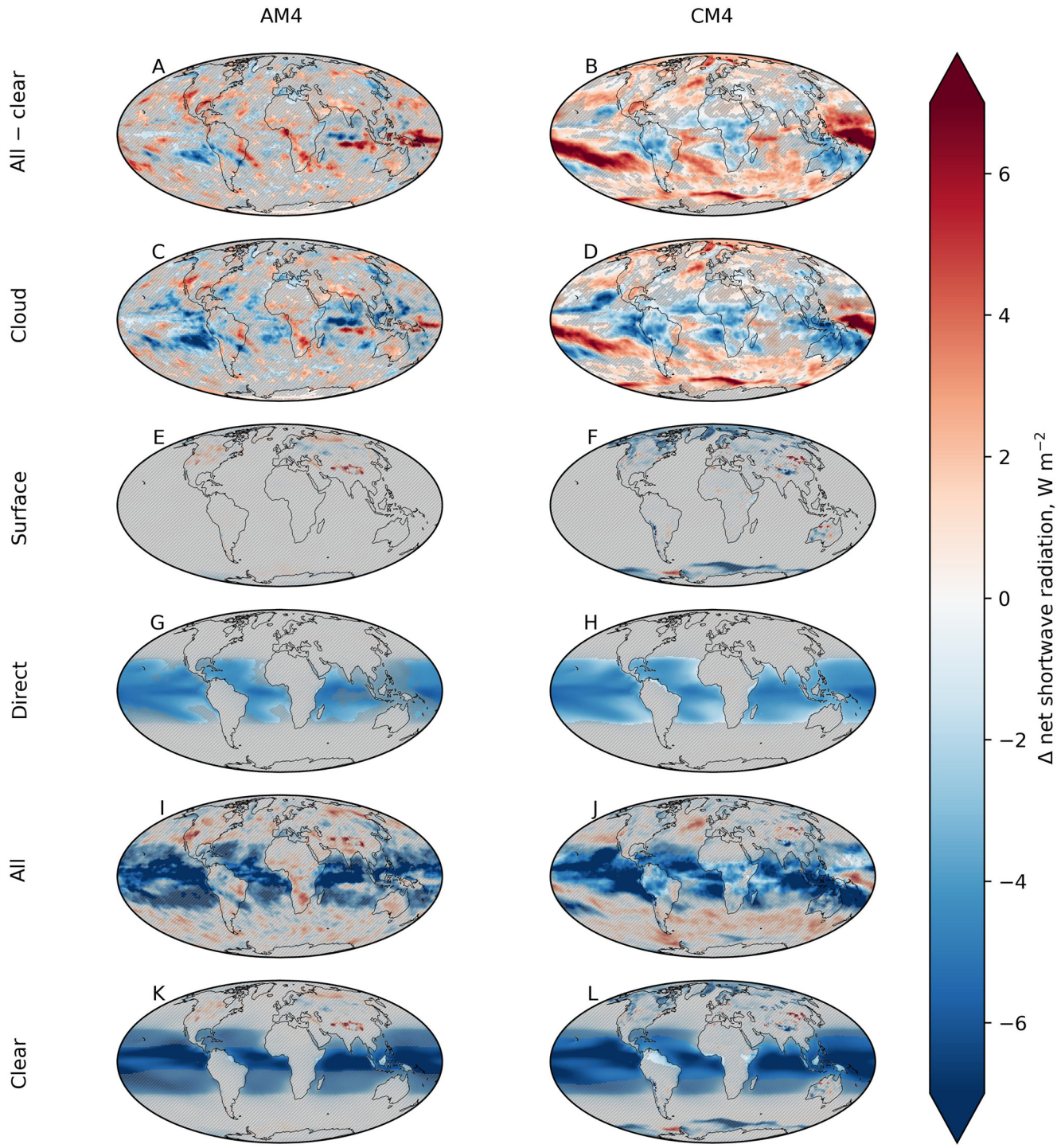

Figure 2. As in Figure 1 but spatially averaged over 2020–2030 for AM4 and 2035–2065 for CM4, with hatched regions corresponding to statistically insignificant differences.

land and throughout the extratropics. The cloud forcing is heterogeneous, while the direct forcing (panels k and g, respectively) is smooth, consistently negative over the tropical oceans but negligible elsewhere. The surface albedo term (panel e) takes nontrivial values only over parts of Tibet, Canada, and Siberia.

We now turn from the effective SWR TOA forcing and its component terms deduced from the fixed-SST AM4 simulations to their responses deduced from the coupled CM4 simulations. The global-mean, annual-mean

SWR TOA anomaly timeseries and its components in CM4 are included in Figure 1, and the time-mean spatial patterns are shown in the right column of Figure 2. These fields reflect both the radiative forcing (including fast, non-SST-mediated adjustments) and the SST-mediated response. For the global-mean fields, interannual fluctuations are larger in the coupled model as expected, but beyond this internal variability, the long-term total SWR TOA response is quite stable and close to the SWR TOA radiative forcing value inferred from AM4. This suggests little SST-mediated SWR TOA response in the all-sky global average.

We note, however, a nontrivial negative trend in the surface albedo contribution (i.e., the surface reflection anomaly is increasing with time), resulting from (and feeding back on) an Arctic-amplified surface temperature response. Despite its tropically confined SSA perturbations, G4sea-salt induces mean cooling relative to SSP245, and various radiative, energetic, and dynamical processes almost inevitably act to amplify the thermal response at high latitudes compared to the global average (Russotto & Biasutti, 2020), concentrated in the Arctic compared to the Antarctic over initial decades (S. A. Hill et al., 2022; Manabe et al., 1991). Central to this is surface albedo feedback due to high-latitude snow and sea-ice changes (Dai et al., 2019).

While the surface albedo contribution increases from AM4 to CM4 (from a global time-mean −0.01 in AM4 to −0.46 W m^{-2} in CM4 over 2035–2065) as well as over time in CM4 runs, the cloud radiative contribution switches sign from the forcing to the response (from global-mean time-mean −0.45 in AM4 to +0.03 W m^{-2} in CM4). A contributing factor in CM4 is an appreciable increase in absorbed SW over much of the Southern Ocean (2b and 2d), coincident with reduced CDNC, LWP, and low cloud fraction (Figure 3ii), to which we now turn.

3.2. Cloud Properties

Three cloud properties are important in studying MCB: CDNC, LWP, and low cloud fraction (Hoffmann & Feingold, 2021). In theory, all three properties would be increased by the imposed aerosol seeding (e.g., Hoffmann & Feingold, 2021; Mülmenstädt et al., 2020). The cloud properties of the AM4 and CM4 simulations are shown in Figure 3 as global-means. As a result of the additional SSA, CDNC increases in both AM4 and CM4 by similar margins. This increase in the cloud droplet concentration is consistent with activation of aerosol indirect effects caused by seeding additional sea salt particles. The increase is especially evident in regions west of continental masses with persistent low-lying cloud decks (a and b in Figure 3ii).

In AM4, the increased CDNC leads to an increase in LWP and low cloud fraction in Figures 3iic and 3iie, respectively. On the other hand, the increase in CDNC in CM4 is associated with a decrease in LWP and low cloud fraction in d and f in Figure 3ii, respectively. The reversal of two cloud properties from AM4 to CM4 is driven mostly by changes in the extratropics and away from marine regions with persistent cloud decks west of continental masses (d and f in Figure 3ii). This depletion of Southern Ocean cloudiness likely stems in part from a decrease in sea salt emissions over much of the region (Figures S1 and S2 in Supporting Information S1), which in turn may be driven to large extent by the large-scale circulation response. Another potential mechanism for the extratropical cloud reductions not involving circulation change is posited by Frazer and Ming (2022): a cooling of the extratropics strengthens the Bergeron-Findeisen process, which would all else equal would act to decrease LWP.

3.3. Regional Response

Regions with persistent low-lying stratocumulus clouds have been suggested as potentially the most effective deployment areas for MCB. To illustrate the regional dependence, we examine the following regions: North Pacific (NP) 10°–30°N, 115°–135°W; South Pacific (SP) 10°S–10°N, 80°–100°W; South Atlantic (SA) 20°S–0°N, 10°E−10°W. In Figure 4, we compare both the radiative components and the cloud properties averaged globally and regionally (only including NP, SP, and SA). In all cases, all cloud properties increase significantly in the regional case compared to the global case. Moreover, both LWP and low clouds do increase regionally in the coupled simulations while decreasing globally.

4. Conclusions

We have presented results from simulations in the GFDL AM4 atmospheric model and the CM4 coupled model following the G4sea-salt protocol of MCB. A −2 W m^{-2} global-mean ERF is obtained in AM4 when SSA emissions are increased by 7.66×10^{-11} kg m^{-2} s^{-1} over all ocean grid points 30°S–30°N. The annual flux increase

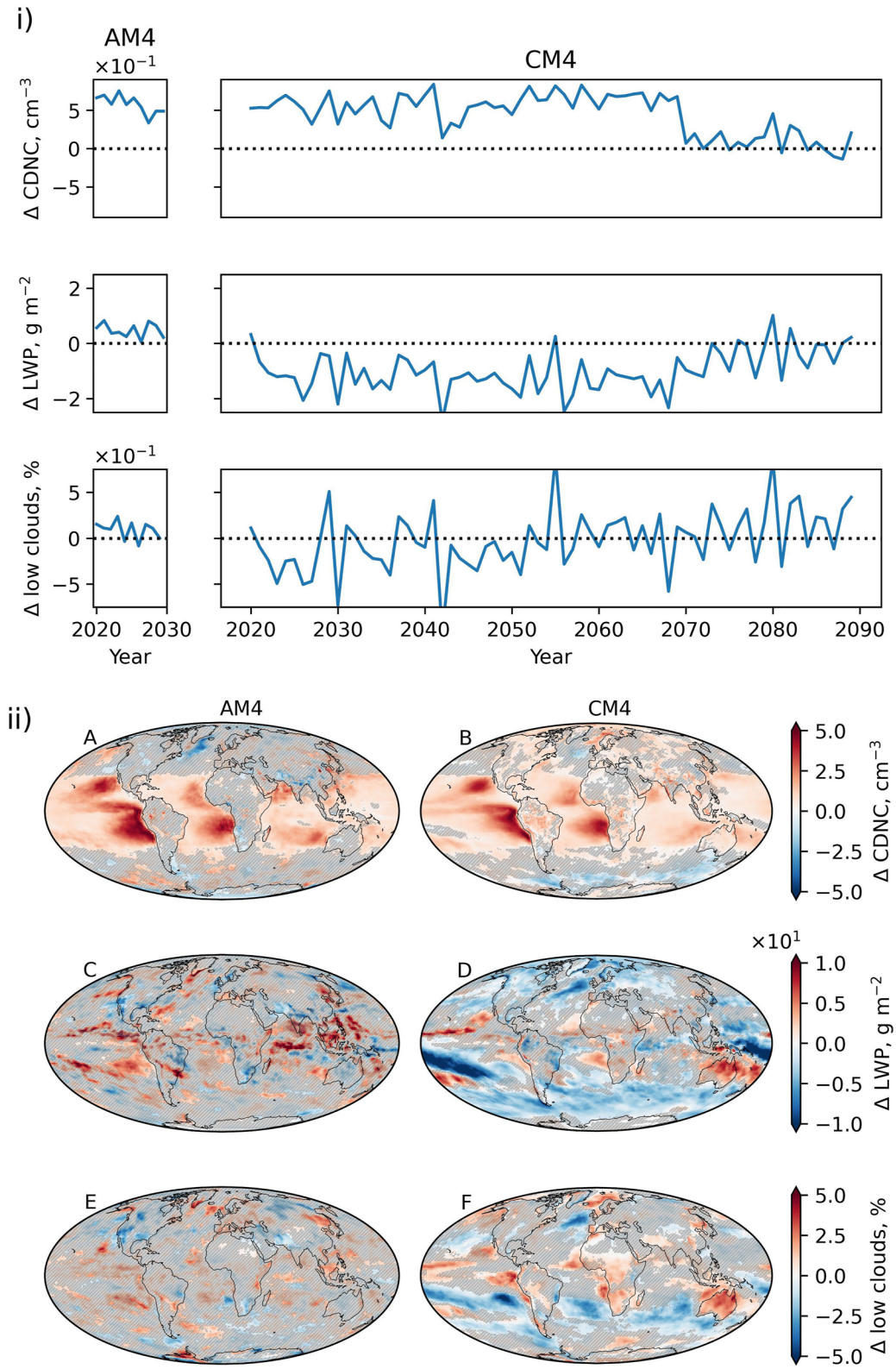

Figure 3. Annual global-mean of cloud droplet number concentration (CDNC), liquid water path (LWP), and low cloud fraction in (i) and their spatial distributions in (ii) averaged over 2020–2030 and 2035–2065 for AM4 and CM4, respectively, with the hatched regions corresponding to statistically insignificant differences.

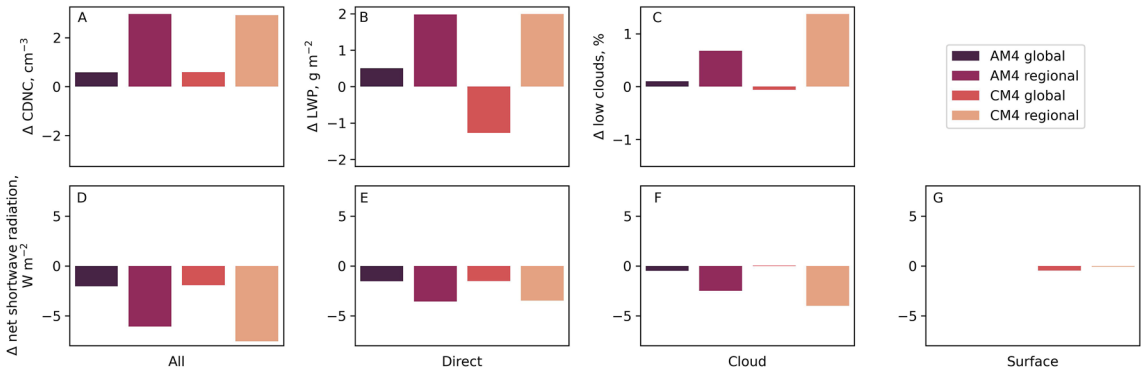

Figure 4. The regional (NP, SP, and SA) and global cloud properties and the Ghan radiative components.

is 456 Tg year^{-1}. Compared to previous studies of G4sea-salt, our results are within range, higher than reported annual fluxes in NorESM1-M and HadGEM2-ES, but lower than GISS-E2-R as reported by Ahlm et al. (2017). Like in GISS-E2-R, we are seeding larger particles, corresponding to the entire submicron range of SSA emissions, which explains the higher flux needed to sustain the radiative offset.

Apart from interannual-scale fluctuations, the radiative and surface thermal responses in CM4 to these imposed sea salt emissions are stable over the 50 years before the emissions modifications are turned off. Afterward, the radiative fields return almost immediately and the surface temperature within a year or so to the trajectory of the SSP2-4.5 case. We show that the resulting -2 W m^2 ERF stems predominantly from the direct scattering effect of the increased SSA burdens, and this direct scattering exhibits little SST-mediated response in the coupled simulation. Conversely, clouds generate a weakly negative contribution to the ERF, but in the coupled response a loss of extratropical clouds results in a net warming rather than cooling contribution in the global-mean.

As with previous studies (Ahlm et al., 2017), the results here indicate a dominant role of the direct radiative effects as seen by the clear-sky component of radiation imbalance as well as following the analysis by Ghan (2013). The ratio of the clear-sky to all-sky components increases appreciably in the coupled simulation as compared to the fixed-SST simulation. This more negative response of the clear-sky component comes exclusively from the extratropics. In the coupled simulation, mean cooling relative to the SSP2-4.5 case triggers Arctic-amplified cooling; this drives increased sea ice extent and Arctic surface albedo, making the clear-sky component of the radiative response more negative.

The cloud response can be inferred from the radiative imbalance components as well as cloud properties. In the fixed-SST simulation, the cloud effects (indirect effects) contribute 25% of the net imbalance (ERF); this contribution to the cooling is also evident in cloud properties (increasing CDNC, LWP, and low cloud fraction due to the additional sea salt emissions). On the other hand, in the coupled simulation, LWP and low cloud fraction decrease, indicating a warming response from clouds; this response can also be seen from the radiative breakdown where the cloud feedbacks in CM4 counterbalance and reverse the indirect effects of forcing in AM4. The balancing happens almost exclusively in the extratropics, where the surface albedo response is more negative in the coupled simulation while the cloud response is more positive.

The dominance of the clear-sky effects in sea salt climate engineering experiments seen here and elsewhere (e.g., Ahlm et al., 2017; Alterskjær et al., 2013; S. Hill & Ming, 2012; Jones & Haywood, 2012; Kravitz et al., 2013) is likely due in part to the unavailability of clouds in the seeding regions and longstanding struggles in simulating enough marine stratocumulus in climate models, especially near the coasts (e.g., see Figure 9 by Zhao et al. [2018a] for the assessment of GFDL's AM4 in predicting CDNC). When juxtaposing the radiation and cloud properties averaged globally and averaged only in regions with persistent low-lying stratocumulus clouds most effective for MCB following S. Hill and Ming (2012), the dominance of the direct effects is diminished. However, the direct component still plays a significant, though not as dominant, role in these regions most appropriate for cloud seeding (Figure 4; e.g., the time-mean global Direct:All ratio is 1.55:2.03 compared to the time-mean regional Direct:All ratio of 3.57:6.07).

The exact size of ideal particles for MCB remains uncertain and will likely depend on local conditions in different places (Hoffmann & Feingold, 2021). The size of seeded particles matters because activating aerosol into cloud

droplets depends on size. The relationship between droplet concentrations and cloud properties such as LWP is nonlinear; for example, Gryspeerdt et al. (2019) report an increase in LWP when increasing CDNC at lower CDNC values, but the trend is reversed when CDNC is higher (LWP decreases with increasing CDNC). Moreover, recent satellite observations and global cloud-resolving model simulations suggest that the LWP response to aerosol perturbation could be either positive, negative, or neutral, depending upon the competing effects of microphysics involved (e.g., Christensen et al., 2022; Hoffmann & Feingold, 2021; Manshausen et al., 2022; Mülmenstädt et al., 2020; Sato et al., 2018; Toll et al., 2019).

Another potential contributor to the predominance of direct scattering over clouds could be the unresolved (as well as uncertain) nature of deep convection in the tropics and its interaction with aerosols. Deep convection and its interaction with seeded aerosol play an important role in determining the LWP and cloud fraction, and therefore the indirect effects (Possner et al., 2020; Schiro et al., 2022). Convective invigoration by aerosols could play a role here, though the scholarly conversation surrounding the topic is ongoing (e.g., Fan & Khain, 2021; Grabowski & Morrison, 2020). Moreover, to achieve the desired cloud brightening, the size of the emitted SSA particles must be small enough as not to cause further precipitation, but at the same time large enough to activate into cloud droplets. In AM4, the added mass of SSA is reapportioned into a prescribed distribution targeting mean phenomena as opposed to perturbed states. As such, we can only ascertain increasing the mass of submicron SSA for the purpose of cloud activation in AM4 and CM4 (Ming et al., 2006, 2007).

A critique of the G4sea-salt protocol is that it does not reflect the reality and practicality of MCB design, for example, deployment will likely be in select regions with select conditions, not the entire marine tropics. Future protocols could benefit from specifying a net negative estimate for the indirect effects, rather than the overall radiative imbalance as well as specifying additional conditions for the deployment regions. Moreover, closer attention to the chemical composition and size of the SSA particles could help to better constrain the indirect effects.

Nonetheless, the G4sea-salt protocol illustrates key challenges in modeling MCB in climate models. Our results indicate that perturbations in the tropics lead to significant changes outside the tropics, for example, the Arctic and in Southern Ocean. In fact, the desired "MCB" cloud effects from G4sea-salt are almost entirely cancelled by feedbacks in the coupled run. Therefore, elucidating relevant feedbacks associated with aerosol–cloud interactions remains a top priority and an obstacle for future modeling efforts of MCB.

Data Availability Statement

Relevant simulations outputs are available at https://10.5281/zenodo.7363892 (Mahfouz, 2022).

Acknowledgments
We thank colleagues at GFDL, especially Leo Donner, Nadir Jeevanjee, David Paynter, Larry Horowitz, and Fabien Paulot, for constructive discussions on versions of this work. This research has been supported by a grant from the Earth's Radiation Budget Initiative, NOAA CPO Climate & CI (Grant 03-01-07-001). This report was prepared by the authors under award NA18OAR4320123 from the National Oceanic and Atmospheric Administration, U.S. Department of Commerce. The statements, findings, conclusions, and recommendations are those of the authors and do not necessarily reflect the views of the National Oceanic and Atmospheric Administration, or the U.S. Department of Commerce.

References

Adcroft, A., Anderson, W., Balaji, V., Blanton, C., Bushuk, M., Dufour, C. O., et al. (2019). The GFDL global ocean and sea ice model OM4.0: Model description and simulation features. *Journal of Advances in Modeling Earth Systems*, *11*, 3167–3211. https://doi.org/10.1029/2019MS001726

Adeniyi, M. O., & Bassey, B. E. I. (2021). Precipitation and temperature response to sea salt injection into low marine clouds over West Africa. *SN Applied Sciences*, *3*(3), 378. https://doi.org/10.1007/s42452-021-04388-9

Ahlm, L., Jones, A., Stjern, C. W., Muri, H., Kravitz, B., & Kristjánsson, J. E. (2017). Marine cloud brightening—As effective without clouds. *Atmospheric Chemistry and Physics*, *17*(21), 13071–13087. https://doi.org/10.5194/acp-17-13071-2017

Alterskjær, K., & Kristjánsson, J. E. (2013). The sign of the radiative forcing from marine cloud brightening depends on both particle size and injection amount. *Geophysical Research Letters*, *40*, 210–215. https://doi.org/10.1029/2012GL054286

Alterskjær, K., Kristjánsson, J. E., Boucher, O., Muri, H., Niemeier, U., Schmidt, H., et al. (2013). Sea-salt injections into the low-latitude marine boundary layer: The transient response in three Earth system models. *Journal of Geophysical Research: Atmospheres*, *118*, 12195–12206. https://doi.org/10.1002/2013JD020432

Christensen, M. W., Gettelman, A., Cermak, J., Dagan, G., Diamond, M., Douglas, A., et al. (2022). Opportunistic experiments to constrain aerosol effective radiative forcing. *Atmospheric Chemistry and Physics*, *22*(1), 641–674. https://doi.org/10.5194/acp-22-641-2022

Dai, A., Luo, D., Song, M., & Liu, J. (2019). Arctic amplification is caused by sea-ice loss under increasing CO_2. *Nature Communications*, *10*(1), 121. https://doi.org/10.1038/s41467-018-07954-9

Fan, J., & Khain, A. (2021). Comments on "Do ultrafine cloud condensation nuclei invigorate deep convection?". *Journal of the Atmospheric Sciences*, *78*(1), 329–339. https://doi.org/10.1175/JAS-D-20-0218.1

Frazer, M. E., & Ming, Y. (2022). Understanding the extratropical liquid water path feedback in mixed-phase clouds with an idealized global climate model. *Journal of Climate*, *35*(8), 2391–2406. https://doi.org/10.1175/JCLI-D-21-0334.1

Ghan, S. J. (2013). Technical Note: Estimating aerosol effects on cloud radiative forcing. *Atmospheric Chemistry and Physics*, *13*(19), 9971–9974. https://doi.org/10.5194/acp-13-9971-2013

Grabowski, W. W., & Morrison, H. (2020). Do ultrafine cloud condensation nuclei invigorate deep convection? *Journal of the Atmospheric Sciences*, *77*(7), 2567–2583. https://doi.org/10.1175/JAS-D-20-0012.1

Gryspeerdt, E., Goren, T., Sourdeval, O., Quaas, J., Mülmenstädt, J., Dipu, S., et al. (2019). Constraining the aerosol influence on cloud liquid water path. *Atmospheric Chemistry and Physics*, *19*(8), 5331–5347. https://doi.org/10.5194/acp-19-5331-2019

Hansen, J. (2005). Efficacy of climate forcings. *Journal of Geophysical Research*, *110*, D18104. https://doi.org/10.1029/2005JD005776
Held, I. M., Guo, H., Adcroft, A., Dunne, J. P., Horowitz, L. W., Krasting, J., et al. (2019). Structure and performance of GFDL's CM4.0 climate model. *Journal of Advances in Modeling Earth Systems*, *11*, 3691–3727. https://doi.org/10.1029/2019MS001829
Hill, S., & Ming, Y. (2012). Nonlinear climate response to regional brightening of tropical marine stratocumulus. *Geophysical Research Letters*, *39*, L15707. https://doi.org/10.1029/2012GL052064
Hill, S. A., Burls, N. J., Fedorov, A., & Merlis, T. M. (2022). Symmetric and antisymmetric components of polar-amplified warming. *Journal of Climate*, *35*(20), 3157–3172. https://doi.org/10.1175/JCLI-D-20-0972.1
Hoffmann, F., & Feingold, G. (2021). Cloud microphysical implications for marine cloud brightening: The importance of the seeded particle size distribution. *Journal of the Atmospheric Sciences*, *78*(10), 3247–3262. https://doi.org/10.1175/JAS-D-21-0077.1
Jones, A., Haywood, J., & Boucher, O. (2009). Climate impacts of geoengineering marine stratocumulus clouds. *Journal of Geophysical Research*, *114*, D10106. https://doi.org/10.1029/2008JD011450
Jones, A., & Haywood, J. M. (2012). Sea-spray geoengineering in the HadGEM2-ES Earth-system model: Radiative impact and climate response. *Atmospheric Chemistry and Physics*, *12*(22), 10887–10898. https://doi.org/10.5194/acp-12-10887-2012
Kim, D.-H., Shin, H.-J., & Chung, I.-U. (2020). Geoengineering: Impact of marine cloud brightening control on the extreme temperature change over East Asia. *Atmosphere*, *11*(12), 1345. https://doi.org/10.3390/atmos11121345
Kravitz, B., Forster, P. M., Jones, A., Robock, A., Alterskjær, K., Boucher, O., et al. (2013). Sea spray geoengineering experiments in the geoengineering model intercomparison project (GeoMIP): Experimental design and preliminary results. *Journal of Geophysical Research: Atmospheres*, *118*, 11175–11186. https://doi.org/10.1002/jgrd.50856
Latham, J., Bower, K., Choularton, T., Coe, H., Connolly, P., Cooper, G., et al. (2012). Marine cloud brightening. *Philosophical Transactions of the Royal Society A: Mathematical, Physical & Engineering Sciences*, *370*(1974), 4217–4262. https://doi.org/10.1098/rsta.2012.0086
Latham, J., & Smith, M. H. (1990). Effect on global warming of wind-dependent aerosol generation at the ocean surface. *Nature*, *347*(6291), 372–373. https://doi.org/10.1038/347372a0
Mahfouz, N. G. A. (2022). The radiative and cloud responses to sea salt aerosol engineering in GFDL models [Dataset]. Zenodo. https://doi.org/10.5281/zenodo.7363892
Manabe, S., Stouffer, R. J., Spelman, M. J., & Bryan, K. (1991). Transient responses of a coupled ocean–atmosphere model to gradual changes of atmospheric CO_2. Part I. Annual mean response. *Journal of Climate*, *4*(8), 785–818. https://doi.org/10.1175/1520-0442(1991)004<0785:TROACO>2.0.CO;2
Manshausen, P., Watson-Parris, D., Christensen, M. W., Jalkanen, J.-P., & Stier, P. (2022). Invisible ship tracks show large cloud sensitivity to aerosol. *Nature*, *610*(7930), 101–106. https://doi.org/10.1038/s41586-022-05122-0
Mårtensson, E. M., Nilsson, E. D., de Leeuw, G., Cohen, L. H., & Hansson, H.-C. (2003). Laboratory simulations and parameterization of the primary marine aerosol production. *Journal of Geophysical Research*, *108*(D9), 4297. https://doi.org/10.1029/2002JD002263
Ming, Y., Ramaswamy, V., Donner, L. J., & Phillips, V. T. J. (2006). A new parameterization of cloud droplet activation applicable to general circulation models. *Journal of the Atmospheric Sciences*, *63*(4), 1348–1356. https://doi.org/10.1175/JAS3686.1
Ming, Y., Ramaswamy, V., Donner, L. J., Phillips, V. T. J., Klein, S. A., Ginoux, P. A., & Horowitz, L. W. (2007). Modeling the interactions between aerosols and liquid water clouds with a self-consistent cloud scheme in a general circulation model. *Journal of the Atmospheric Sciences*, *64*(4), 1189–1209. https://doi.org/10.1175/JAS3874.1
Monahan, E. C., Spiel, D. E., & Davidson, K. L. (1986). A model of marine aerosol generation via whitecaps and wave disruption. In E. C. Monahan & G. M. Niocaill (Eds.), *Oceanic whitecaps: And their role in air–sea exchange processes* (pp. 167–174). Springer Netherlands. https://doi.org/10.1007/978-94-009-4668-2_16
Mülmenstädt, J., Nam, C., Salzmann, M., Kretzschmar, J., L'Ecuyer, T. S., Lohmann, U., et al. (2020). Reducing the aerosol forcing uncertainty using observational constraints on warm rain processes. *Science Advances*, *6*(22), eaaz6433. https://doi.org/10.1126/sciadv.aaz6433
National Academies of Sciences, Engineering, and Medicine. (2021). *Reflecting sunlight: Recommendations for solar geoengineering research and research governance*. National Academies Press. https://doi.org/10.17226/25762
Partanen, A.-I., Kokkola, H., Romakkaniemi, S., Kerminen, V.-M., Lehtinen, K. E. J., Bergman, T., et al. (2012). Direct and indirect effects of sea spray geoengineering and the role of injected particle size. *Journal of Geophysical Research*, *117*, D02203. https://doi.org/10.1029/2011JD016428
Paulot, F., Paynter, D., Winton, M., Ginoux, P., Zhao, M., & Horowitz, L. W. (2020). Revisiting the impact of sea salt on climate sensitivity. *Geophysical Research Letters*, *47*, e2019GL085601. https://doi.org/10.1029/2019GL085601
Possner, A., Eastman, R., Bender, F., & Glassmeier, F. (2020). Deconvolution of boundary layer depth and aerosol constraints on cloud water path in subtropical stratocumulus decks. *Atmospheric Chemistry and Physics*, *20*(6), 3609–3621. https://doi.org/10.5194/acp-20-3609-2020
Rasch, P. J., Latham, J., & Chen, C.-C. J. (2009). Geoengineering by cloud seeding: Influence on sea ice and climate system. *Environmental Research Letters*, *4*(4), 045112. https://doi.org/10.1088/1748-9326/4/4/045112
Rossow, W. B., & Schiffer, R. A. (1999). Advances in understanding clouds from ISCCP. *Bulletin of the American Meteorological Society*, *80*(11), 2261–2287. https://doi.org/10.1175/1520-0477(1999)080<2261:AIUCFI>2.0.CO;2
Rotstayn, L. D. (1997). A physically based scheme for the treatment of stratiform clouds and precipitation in large-scale models. I: Description and evaluation of the microphysical processes. *Quarterly Journal of the Royal Meteorological Society*, *123*(541), 1227–1282. https://doi.org/10.1002/qj.49712354106
Rotstayn, L. D. (2005). A smaller global estimate of the second indirect aerosol effect. *Geophysical Research Letters*, *32*, L05708. https://doi.org/10.1029/2004GL021922
Rotstayn, L. D., Ryan, B. F., & Katzfey, J. J. (2000). A scheme for calculation of the liquid fraction in mixed-phase stratiform clouds in large-scale models. *Monthly Weather Review*, *128*(4), 1070–1088. https://doi.org/10.1175/1520-0493(2000)128<1070:ASFCOT>2.0.CO;2
Russotto, R. D., & Biasutti, M. (2020). Polar amplification as an inherent response of a circulating atmosphere: Results from the TRACMIP aquaplanets. *Geophysical Research Letters*, *47*(6), e2019GL086771. https://doi.org/10.1029/2019GL086771
Sato, Y., Goto, D., Michibata, T., Suzuki, K., Takemura, T., Tomita, H., & Nakajima, T. (2018). Aerosol effects on cloud water amounts were successfully simulated by a global cloud-system resolving model. *Nature Communications*, *9*(1), 985. https://doi.org/10.1038/s41467-018-03379-6
Schiro, K. A., Su, H., Ahmed, F., Dai, N., Singer, C. E., Gentine, P., et al. (2022). Model spread in tropical low cloud feedback tied to overturning circulation response to warming. *Nature Communications*, *13*(1), 7119. https://doi.org/10.1038/s41467-022-34787-4
Sherwood, S. C., Webb, M. J., Annan, J. D., Armour, K. C., Forster, P. M., Hargreaves, J. C., et al. (2020). An assessment of Earth's climate sensitivity using multiple lines of evidence. *Reviews of Geophysics*, *58*, e2019RG000678. https://doi.org/10.1029/2019RG000678
Shin, H. H., Ming, Y., Zhao, M., Chen, X., & Lin, S.-J. (2019). Improved surface layer simulation using refined vertical resolution in the GFDL atmospheric general circulation model. *Journal of Advances in Modeling Earth Systems*, *11*, 905–917. https://doi.org/10.1029/2018MS001437

Spada, M., Jorba, O., Pérez García-Pando, C., Janjic, Z., & Baldasano, J. M. (2013). Modeling and evaluation of the global sea-salt aerosol distribution: Sensitivity to size-resolved and sea-surface temperature dependent emission schemes. *Atmospheric Chemistry and Physics*, *13*(23), 11735–11755. https://doi.org/10.5194/acp-13-11735-2013

Stjern, C. W., Muri, H., Ahlm, L., Boucher, O., Cole, J. N. S., Ji, D., et al. (2018). Response to marine cloud brightening in a multi-model ensemble. *Atmospheric Chemistry and Physics*, *18*(2), 621–634. https://doi.org/10.5194/acp-18-621-2018

Stocker, T. (Ed.), (2014). *Climate change 2013: The physical science basis: Working Group I contribution to the Fifth assessment report of the Intergovernmental Panel on Climate Change*. Cambridge University Press.

Tang, I. N., Tridico, A. C., & Fung, K. H. (1997). Thermodynamic and optical properties of sea salt aerosols. *Journal of Geophysical Research*, *102*(D19), 23269–23275. https://doi.org/10.1029/97JD01806

Toll, V., Christensen, M., Quaas, J., & Bellouin, N. (2019). Weak average liquid–cloud–water response to anthropogenic aerosols. *Nature*, *572*(7767), 51–55. https://doi.org/10.1038/s41586-019-1423-9

Welch, B. L. (1947). The generalization of 'student's' problem when several different population varlances are involved. *Biometrika*, *34*(1–2), 28–35. https://doi.org/10.1093/biomet/34.1-2.28

Wood, R. (2021). Assessing the potential efficacy of marine cloud brightening for cooling Earth using a simple heuristic model. *Atmospheric Chemistry and Physics Discussions*, *21*, 14507–14533. https://doi.org/10.5194/acp-2021-327

Zhao, M., Golaz, J.-C., Held, I. M., Guo, H., Balaji, V., Benson, R., et al. (2018a). The GFDL global atmosphere and land model AM4.0/LM4.0: 1. Simulation characteristics with prescribed SSTs. *Journal of Advances in Modeling Earth Systems*, *10*, 691–734. https://doi.org/10.1002/2017MS001208

Zhao, M., Golaz, J.-C., Held, I. M., Guo, H., Balaji, V., Benson, R., et al. (2018b). The GFDL global atmosphere and land model AM4.0/LM4.0: 2. Model description, sensitivity studies, and tuning strategies. *Journal of Advances in Modeling Earth Systems*, *10*, 735–769. https://doi.org/10.1002/2017MS001209

Zhu, Y., Zhang, Z., & Crabbe, M. J. C. (2021). Extreme climate response to marine cloud brightening in the arid Sahara-Sahel-Arabian Peninsula zone. *International Journal of Climate Change Strategies and Management*, *13*, (3), 250–265. https://doi.org/10.1108/IJCCSM-06-2020-0051